Phosphatidylinositol 4-phosphate 5-kinase alpha (PIPKα) regulates neuronal microtubule depolymerase kinesin, KIF2A and suppresses elongation of axon branches

Yasuko Noda[a,1], Shinsuke Niwa[a,1], Noriko Homma[a], Hiroyuki Fukuda[b], Shinobu Imajo-Ohmi[b], and Nobutaka Hirokawa[a,c,2]

[a]Department of Cell Biology, Graduate School of Medicine, University of Tokyo, Bunkyo-ku, Tokyo 113-0033, Japan; [b]Institute of Medical Science, University of Tokyo, Minato-ku, Tokyo 108-8639, Japan; and [c]Center of Excellence in Genomic Medicine Research, King Abdulaziz University, Jeddah 21589, Saudi Arabia

Neuronal morphology is regulated by cytoskeletons. Kinesin superfamily protein 2A (KIF2A) depolymerizes microtubules (MTs) at growth cones and regulates axon pathfinding. The factors controlling KIF2A in neurite development remain totally elusive. Here, using immunoprecipitation with an antibody specific to KIF2A, we identified phosphatidylinositol 4-phosphate 5-kinase alpha (PIPKα) as a candidate membrane protein that regulates the activity of KIF2A. Yeast two-hybrid and biochemical assays demonstrated direct binding between KIF2A and PIPKα. Partial colocalization of the clusters of punctate signals for these two molecules was detected by confocal microscopy and photoactivated localization microscopy. Additionally, the MT-depolymerizing activity of KIF2A was enhanced in the presence of PIPKα in vitro and in vivo. PIPKα suppressed the elongation of axon branches in a KIF2A-dependent manner, suggesting a unique PIPK-mediated mechanism controlling MT dynamics in neuronal development.

kinesin-13 | KIF | PIP5K | PIP2

During brain development, neurons must extend their axons and dendrites into the proper target regions. This is achieved through dynamic control of cytoskeletal components such as actin filaments and microtubules (MTs). Kinesin superfamily protein 2A (KIF2A), a member of the kinesin-13 family, is a critical regulator of MT dynamics in axon pathfinding. Among the many kinesin superfamily proteins, kinesin-13 family members have MT-depolymerizing activity (1–4). KIF2A is enriched in the developing brain; it is localized predominantly in growth cones and decouples successive tubulin dimers from the tips of MTs (5–8). MTs become abnormally stable at $Kif2a^{-/-}$ growth cones, resulting in extended axon branches (9). However, it remains unknown what factors regulate KIF2A during neuronal development. To this end, we searched for a binding protein of KIF2A in the developing brain, which led us to identify a key signaling enzyme, phosphatidylinositol 4-phosphate 5-kinase alpha (PIPKα).

Recent advances in cell signaling have elucidated the widespread involvement of phosphatidylinositide derivatives in intracellular processes, which are strictly controlled both spatially and temporally by the balance between kinase and phosphatase activities (10–12). Among such enzymes, PIPK, which phosphorylates the 5 position of phosphatidylinositol 4-phosphate, produces phosphatidylinositol 4,5-bisphosphate (PIP_2) and also supplies the substrate for phosphatidylinositol 1,4,5-triphosphate (PIP_3). Three subtypes of PIPK have been identified in mammals (13–15). As the different nomenclature of PIPK in mouse and human is confusing, we use in this manuscript the human terminology set by the Human Genome Project (http://www.ornl.gov/sci/techresources/Human_Genome/home.shtml). Three subtypes are designated PIPKα (PIP5K1A), PIPKβ (PIP5K1B), and PIPKγ (PIP5K1C). The three PIPK members have a similar catalytic core domain and unique head and tail domains. PIPKα and PIPKβ have very similar structures but PIPKγ has a longer C-terminal domain. Whereas PIPKγ regulates synaptic-vesicle biogenesis, PIP_2 production by PIPKβ stabilizes cortical actin filaments through actin-associated proteins such as

α-actinin, gelsolin, and profilin, and stimulates redistribution of focal adhesion proteins, leading to the inhibition of neurite elongation (16–20). Thus, PIPK acts as a negative regulator of neurite formation. Although MT networks must also be dynamically modulated when neurite elongation is inhibited (9), it is not known how PIPK regulates MT dynamics. In the present study, we found that the direct association of PIPKα with KIF2A augmented the MT-depolymerizing activity of KIF2A in vitro and in vivo.

Results

PIPKα Coimmunoprecipitates with KIF2A. KIF2A is enriched in growing neurites in the molecular layer of the juvenile cerebellum (6). To identify the regulators of KIF2A, we purified KIF2A from postnatal day 7 (P7) mouse cerebellum and analyzed the purified fraction by mass spectrometry and Western blotting. We found that PIPKα (also known as murine PIPKβ) reproducibly coimmunoprecipitated with KIF2A (Fig. 1A, Left). PIPKα remained in the immunoprecipitated fraction even after detergent extraction (Fig. 1A, Right), suggesting a possibility that PIPKα coimmunoprecipitated with KIF2A through direct binding. Inversely, when immunoprecipitation was conducted using anti-PIPKα antibody in the presence of 1% Triton X-100, KIF2A was copurified with PIPKα (Fig. 1B, Left). Additional immunoprecipitation using anti-PIPKγ antibody did not copurify KIF2A (Fig. 1B, Right), confirming the specific binding between KIF2A and PIPKα.

Direct Interaction Between PIPKα and KIF2A in Vitro. Because immunoprecipitation in the presence of detergent suggested the direct interaction between KIF2A and PIPKα, we tested this binding with yeast two-hybrid experiments using several deletion constructs (Fig. 1C). Results demonstrated a direct interaction between PIPKα and an N-terminal fragment of KIF2A containing the neck region (Nt+Neck) (Fig. 1D, asterisk). Neither negative control vector (pGADT7 vector) nor PIPKγ vector gave positive signals in this experiment. Next, an *Escherichia coli* expression system using purified KIF2A-(His)$_6$ and GST-PIPKα was used to test the association. Results showed that KIF2A-(His)$_6$ was copurified with GST-PIPKα (Fig. 1E, asterisk). To confirm this result and more precisely identify the binding domain, successive deletion constructs of KIF2A were prepared for in vitro binding assays (Fig. 1F). The deletion mutants and either GST or GST-PIPKα were mixed, incubated, and then purified with glutathione beads. The full-length, Nt+Neck region, and neck-only region (Neck) of KIF2A were copurified with GST-PIPKα but not with
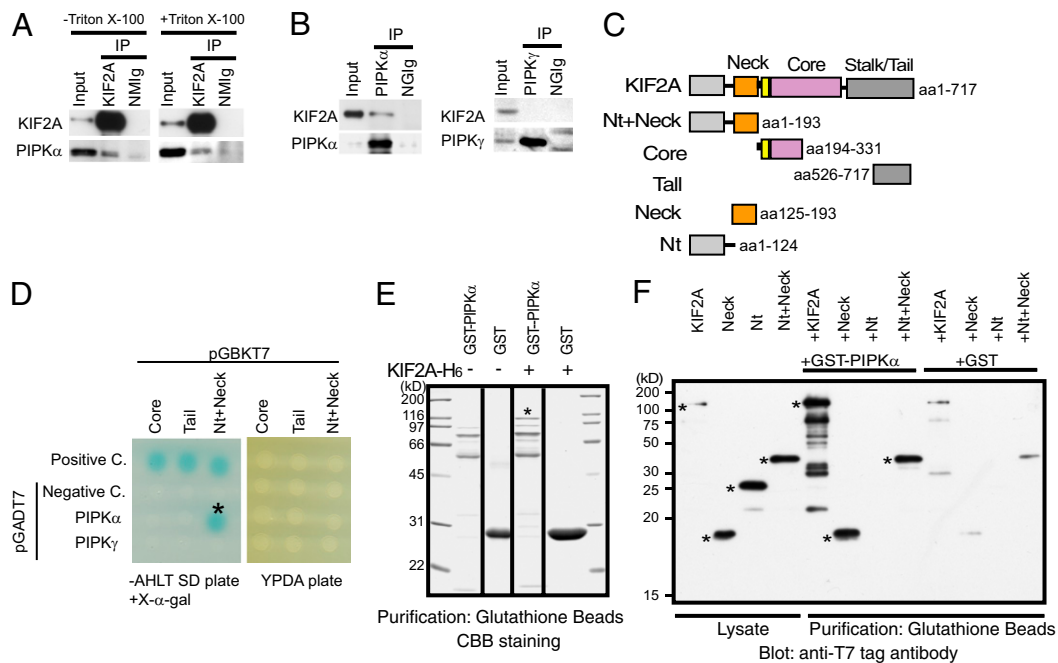
NEUROSCIENCE

Fig. 1. Identification of a direct interaction between KIF2A and PIPKα. (*A* and *B*) Western blot analysis of fractions immunoprecipitated by anti-KIF2A (*A*) and anti-PIPKα or anti-PIPKγ (*B*) antibodies. Immunoprecipitation (IP) by the anti-KIF2A antibody was performed with (+) or without (–) 1% Triton X-100. The S2 fraction including 30 μg of protein (Input), or the eluted fraction corresponding to 0.5 μg of anti-KIF2A antibody (KIF2A), anti-PIPKα antibody (PIPKα), anti-PIPKγ antibody (PIPKγ), normal mouse IgG (NMIg), or normal goat IgG (NGIg), was loaded in each lane. (*C*) Constructs of KIF2A used for the assays. (*D*) Yeast two-hybrid analyses of the direct interactions between baits and preys. pCL1, an expression vector for full-length GAL4, and pGADT7 vectors were used for the positive and negative control (Positive C. and Negative C.), respectively. Transformants were plated on SD agar plates without adenine, histidine, leucine, and tryptophan (−AHLT) supplemented with X-α-gal (*Left*) and YPDA agar plate (*Right*). (*E*) In vitro binding assays. KIF2A-(His)$_6$ (asterisk) bound specifically to GST-PIPKα–conjugated beads but not to GST-conjugated beads. (*F*) Western blot analysis with anti-T7 tag antibody of binding assay reactions using deletion constructs of KIF2A. Each fragment is indicated in *C*. KIF2A proteins are indicated by asterisks.

GST. Thus, the neck domain of KIF2A was identified as the PIPKα-binding domain (Fig. 1*F*).

Colocalization of KIF2A and PIPKα at the Tips of Neurites. To examine the physiological relevance of the interaction between KIF2A and PIPKα, the localization of these two molecules was observed in cultured hippocampal neurons. Hippocampal neurons at 3 d in vitro (div) were fixed, doubly stained with anti-KIF2A and anti-PIPKα antibodies, and observed using a confocal microscope.

Colocalization of KIF2A and PIPKα was found at the tips of neurites (Fig. 2*A*, arrows). The specificity of anti-PIPKα antibody was checked by blocking using purified PIPKα and PIPKγ proteins (Fig. S1). The specificity of anti-KIF2A has been checked in previous studies (6, 9).

To observe the colocalization of KIF2A and PIPKα at higher resolution, we used photoactivated localization microscopy (PALM), which can detect photoactivated stochastic images of molecules with a resolution of ~10 nm. Scanned images of both
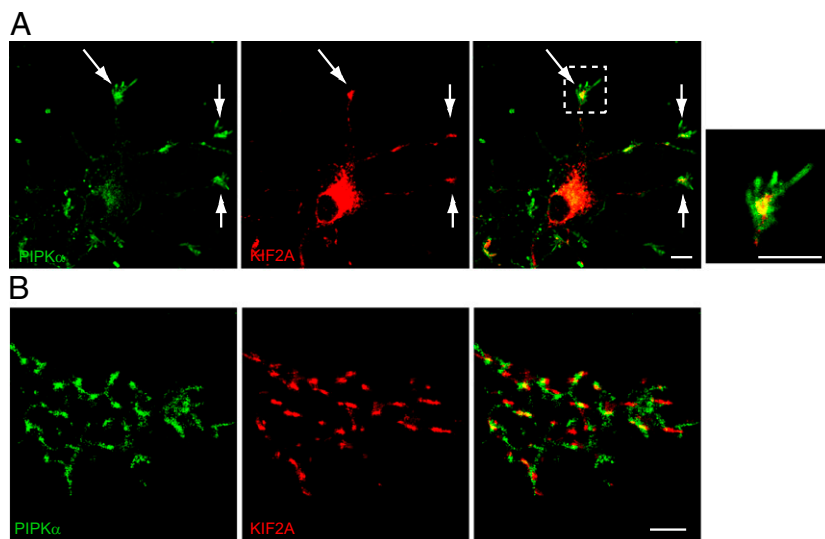

Fig. 2. Endogenous localization of KIF2A and PIPKα. (*A*) Fluorescence images of cultured developing hippocampal neurons at 3 div double-stained with anti-KIF2A (red) and anti-PIPKα (green) antibodies. (*Right*) The boxed area is zoomed. KIF2A and PIPKα accumulated at the tips of neurites (arrows) and partially colocalized in growth cones. (Scale bars, 10 μm.) (*B*) Reconstructed signals for KIF2A and PIPKα in the growth cones detected by PALM. Fluorescence images of cultured developing hippocampal neurons at 3 div double-stained with anti-KIF2A (red) and anti-PIPKα (green) antibodies. (Scale bar, 1 μm.)

KIF2A and PIPKα showed clustered patterns in growth cones, which substantially overlapped when reconstructed (Fig. 2B; 59 ± 12% of KIF2A-positive clusters colocalized with PIPKα-positive clusters in the growth cones; $n = 40$). Because the PALM images were taken using total internal reflection fluorescent microscopy (TIRF), the depth of these images was within 100 nm. Considering the biochemical data showing direct binding (Fig. 1), KIF2A and PIPKα would bind near the plasma membrane.

PIPKα Accelerates the MT-Depolymerizing Activity of KIF2A in Vitro. Previous studies have shown that PIPK indirectly controls actin dynamics through PIP_2 signaling. However, the direct interaction between PIPKα and the neck region of KIF2A, which is critical for its activity, hinted that PIPKα might directly activate KIF2A (21–26). First, MT-depolymerizing activity of KIF2A, PIPKα, and PIPKγ was observed using guanosine 5′-[(α,β)-methyleno] triphosphate (GMPCPP)-stabilized MTs. MT depolymerization was tested by ultracentrifugation and subsequent SDS/PAGE stained with Coomassie brilliant blue (CBB). In this experiment, the supernatant and the pellet fractions represent tubulin dimers and polymerized MTs, respectively. Consequently, whereas 100 nM PIPKα, PIPKγ, and BSA did not show MT-depolymerizing activity, 100 nM GST-KIF2A induced MT depolymerization (Fig. 3A). Addition of 5 mM adenosine 5′-(β,γ-imino) triphosphate (AMP-PNP), an ATP analog that inhibits the ATPase activity of KIFs, inhibited the MT-depolymerizing activity of GST-KIF2A (Fig. 3A).

To test whether PIPKα enhances the MT-depolymerizing activity of KIF2A or not, GMPCPP-stabilized and tetramethylrhodamine (TMR)-labeled MTs were used as a substrate and the effect of PIPKα was directly observed by microscopy. We determined to use a low concentration of KIF2A (15 nM) in this experiment because a high concentration (100 nM) of KIF2A completely depolymerized MTs (Fig. 3A). When MTs were treated with both 15 nM KIF2A and either 100 nM BSA or PIPKγ for 20 min, MTs became shorter but significant amounts of short MTs remained (Fig. 3B, Left and Right). In contrast, when MTs were incubated with both 15 nM KIF2A and 100 nM PIPKα for 20 min, MTs were almost completely diminished (Fig. 3B, Center). Without KIF2A, MTs were intact after the incubation (Fig. 3B, Insets). This result suggests that MT-depolymerizing activity of KIF2A is enhanced by the presence of PIPKα.

To quantitatively compare them, MTs were treated with various concentrations of KIF2A in the presence of either 100 nM BSA, PIPKα, or PIPKγ and, subsequently, ultracentrifugation, SDS/PAGE, and CBB staining were performed. KIF2A showed dose-dependent MT-depolymerizing activity that had a sigmoidal pattern (Fig. 3C). The presence of PIPKα, but not PIPKγ, in the reaction significantly increased the supernatant:total ratio of tubulin,

compared with the presence of BSA. Using these data, the EC_{50}, indicating the concentration of KIF2A that gives 50% MT polymer and 50% tubulin heterodimer, was calculated using Eq. 1 as described (27) (Fig. 3D and Materials and Methods). As a result, the EC_{50} of GST-KIF2A was, respectively, 5.1 ± 0.5 nM, 12.1 ± 0.6 nM, and 11.3 ± 0.4 nM in the presence of PIPKα, BSA, and PIPKγ (mean ± SD, $n = 3$, $P < 0.01$, Student's t test), suggesting that the presence of PIPKα, but not PIPKγ, activated KIF2A.
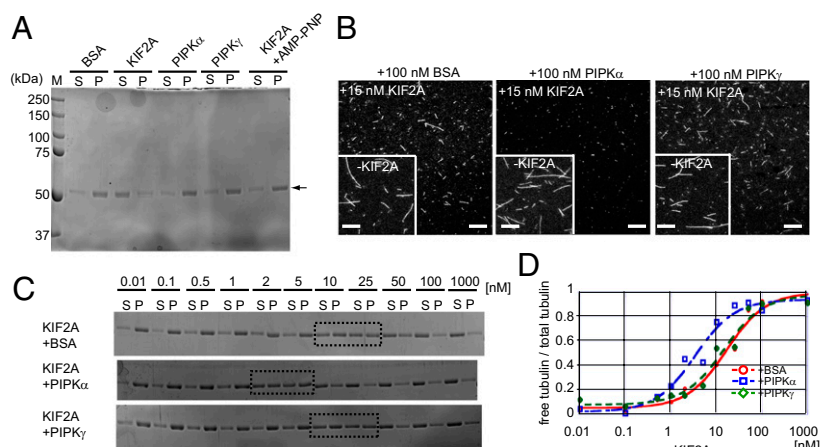
Morphological Similarity Between PIPKα Knockdown and KIF2A Knockout. Because KIF2A suppresses the elongation of axon branches in hippocampal neurons and because previous studies have shown that overexpression of PIPKβ, an isoform of PIPKα, inhibits neurite formation (19, 20), we studied the role of PIPKα in developing hippocampal neurons. First, the effect of PIPKα knockdown was examined. MicroRNA (miRNA) vectors were designed to knock down PIPKα. In this experiment, EGFP was inserted as a marker into these vectors to observe the cell morphology (Fig. 4A, schema). The knockdown effect was examined using N1E-115 cells. Western blotting showed that the amount of PIPKα was reduced by ∼50% by their respective miRNA vectors (Fig. 4A, Western blot). As the transfection efficiency was about 60%, we estimate the knockdown efficiency of these vectors to be over 80% in each transfected cell.

Typical wild-type neurons at 3 div have multiple dendrites and a long axon. From the axon, very short collaterals were branched (Fig. 4B, WT). miRNA vectors were transfected to WT neurons when cells were plated, and cultured for 3 d. As a consequence, the lengths of axon branches became significantly longer (Fig. 4 B–D, WT+PIPKαKD), which is very similar to the phenotype of $Kif2a^{-/-}$ neurons (Fig. 4 B–D, KO). In contrast, dendrite numbers and lengths were not significantly affected by loss of function of either PIPKα or KIF2A. These results suggest that, similar to KIF2A, PIPKα suppresses the formation of axon branches in developing hippocampal neurons. Because no morphological differences were statistically observed between PIPKα-knockdown neurons and $Kif2a^{-/-}$ neurons, PIPKα and KIF2A might work in the same pathway. To confirm this, PIPKα was knocked down in $Kif2a^{-/-}$ background. Accordingly, cellular morphology of PIPKα-knockdown $Kif2a^{-/-}$ neurons was not significantly changed compared with control $Kif2a^{-/-}$ neurons (Fig. 4 B–D, KO+PIPKαKD). Thus, PIPKα and KIF2A are thought to work in the same pathway.

Overexpression of PIPKα Inhibits Axon Elongation via KIF2A. It has been shown that PIPKβ overexpression inhibits neurite formation in N1E-115 neuroblastoma (19, 20). Therefore, we tested whether PIPKα also has this activity. N1E-115 neuroblastoma cells were cotransfected with pEGFP vector and either pECFP or pECFP-PIPKα and differentiated for 24 h, and the cell morphology was

Fig. 3. PIPKα enhances MT depolymerization induced by KIF2A. (A) SDS/PAGE and Coomassie brilliant blue staining of MT-depolymerizing assay products. GMPCPP-stabilized MTs (1 µM) were incubated with the indicated proteins purified from E. coli in the presence of MgATP for 20 min at 22 °C. Equal volumes of supernatant (S) and pellet (P) fractions represent tubulin dimers and MT polymers, respectively. Representative data from three independent experiments are shown. (B) MT depolymerization observed by fluorescent microscopy. GMPCPP-stabilized and TMR-labeled MTs were incubated with 15 nM KIF2A and either 100 nM BSA, PIPKα, or PIPKγ for 20 min at 22 °C and observed by confocal microscopy. (Insets) Negative control experiments conducted in the absence of KIF2A (−KIF2A). (Scale bars, 10 µm.) (C and D) MT-depolymerizing activity of various concentrations of KIF2A in the presence of 100 nM BSA, PIPKα, or PIPKγ. (C) SDS/PAGE stained with CBB is shown. A representative result from three independent experiments is shown. (D) Representative data derived from three independent experiments are fit to the dose–response curve (Eq. 1).

examined using GFP signal. Similar to the results for PIPKβ overexpression, it was shown that PIPKα overexpression before differentiation also inhibited neurite elongation in N1E-115 cells (Fig. S2; 98.6 ± 34.5 μm and 37.4 ± 23.1 μm, CFP-expressing cells and CFP-PIPKα–expressing cells, respectively, mean ± SD, P < 0.01, Student's t test). Next, we conducted overexpression experiments in hippocampal neurons. Hippocampal neurons were transfected with EGFP vector and either ECFP (negative control) or ECFP-PIPKα at 2 div and cultured for 24 h, and then the cell morphology was examined using GFP signal (Fig. 5A). Similar to N1E-115, axons were significantly shorter in PIPKα-overexpressing neurons than those of the negative control neurons (Fig. 5, +PIPKα). To demonstrate that KIF2A is required for this process, PIPKα was overexpressed in $Kif2a^{-/-}$ background. Results showed that PIPKα overexpression in $Kif2a^{-/-}$ background did not change cellular morphology (Fig. 5, KO+PIPKα), suggesting that KIF2A is required for the function of PIPKα.

Overexpression of PIPKα Induces MT Depolymerization in Neurites. Previous studies have shown that PIPK regulates the dynamics of actin filaments. The above results suggested a possibility that PIPK also regulates MT dynamics in neurites via KIF2A (Figs. 1–5). Hence, we next examined MT dynamics in growth cones in PIPKα-overexpressed WT and $Kif2a^{-/-}$ neurons and PIPKα-knockdown WT and $Kif2a^{-/-}$ neurons. EGFP-EB3 was used as a probe for the plus ends of MTs (28). In this experiment, miRNA vectors without an EGFP cassette were used. As a result, we were able to observe MT dynamics in growth cones (Fig. 6 and Movies S1, S2, S3, S4, S5, and S6). For analysis, we classified MT dynamics into three patterns: (*i*) collision and depolymerization, (*ii*) turning, and (*iii*) depolymerization without collision (Fig. 6A). In WT neurites, MT tips often shrank immediately after collision with the plasma membrane (Fig. 6 *A* and *B* and Movie S1). However, in PIPKα-overexpressing WT neurites, the MT tips tended to shrink before attaching to the plasma membrane (Fig. 6 *A* and *B* and Movie S2). In PIPKα-knockdown WT neurites, MTs often collided with the plasma membrane and tended to turn (Fig. 6 *A* and *C* and Movie S3). In $Kif2a^{-/-}$ neurons, turned MTs are more often observed than in WT neurons, as reported previously (9) (Fig. 6 *A* and *C* and Movie S4). Statistically, no difference was observed between $Kif2a^{-/-}$ neurons and PIPKα-

knockdown WT neurons. In contrast to WT neurons, neither PIPKα overexpression nor PIPKα knockdown changed the MT dynamics in $Kif2a^{-/-}$ neurons (Fig. 6 and Movies S5 and S6), which is very similar to the result of neuronal morphology (Fig. 4). These observations are consistent with the in vitro experiments showing that PIPKα did not directly depolymerize MTs but did augment the MT-depolymerizing activity of KIF2A (Fig. 3).

To investigate further the functional link between PIPKα and KIF2A in neurites, PIPKα, KIF2A, or both were transfected into differentiated N1E-115 cells and the neurite length was compared (Fig. S3). Neurite length in PIPKα-expressing neurons was shorter than in the negative control. Although neurite lengths in KIF2A-expressing cells were not significantly changed, neurite length in both KIF2A- and PIPKα-expressing cells was much shorter than that of only PIPKα-expressing cells (Fig. S3B), suggesting that KIF2A and PIPKα cooperatively work to control neurite length.

Discussion

Recently, it has been revealed that kinesin superfamily motor proteins work not only as intracellular transporters but also as regulators of MT dynamics (1, 3, 29, 30). Among them, KIF2A is known as an MT depolymerase in neurons, although its regulation mechanisms remain totally elusive. It is well-established that PIPK controls actin dynamics by producing PIP$_2$. Previous studies have shown a role for PIPKβ (murine PIPKα) as a negative regulator of neurite formation in N1E-115 neuroblastoma cells and early-stage hippocampal neurons (17, 19, 20). In this study, we show that PIPKα, which is structurally very similar to PIPKβ, also suppresses neurite elongation in N1E-115 neuroblastoma cells and developing hippocampal neurons (Fig. 5 and Fig. S2). Knockdown and overexpression experiments collectively suggested that PIPKα controls the length of axon collaterals in hippocampal neurons (Figs. 4 and 5). Interestingly, MT dynamics were changed in PIPKα-overexpressing and -knockdown neurons (Fig. 6). It is known that PIPKα is a plasma membrane-associated protein and KIF2A is a cytosolic protein that interacts with MT tips (31, 32). However, it is thought that the chance that they associate is not small because our live-cell imaging using the GFP-EB3 probe showed that MT tips often collided with the plasma membrane in growth cones (Movies S1, S2, S3, S4, S5, and S6). Truly, their colocalization was observed near the plasma membrane of growth
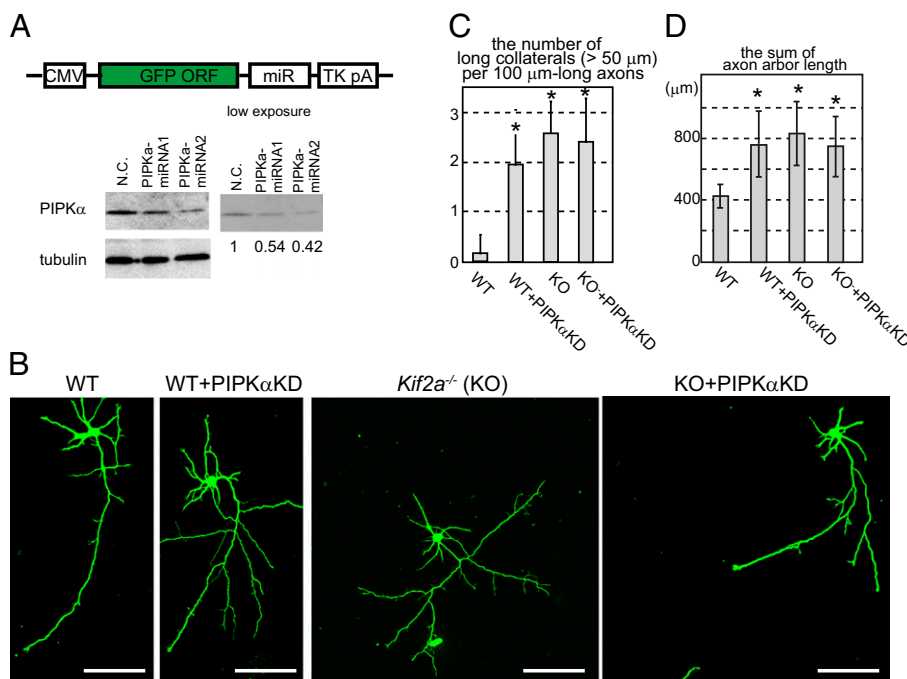
A

B

WT   WT+PIPKαKD   *Kif2a^{-/-}* (KO)   KO+PIPKαKD

C

the number of long collaterals (> 50 μm) per 100 μm-long axons

D

the sum of axon arbor length

Fig. 4. Morphological phenotypes in PIPKα-knockdown and/or KIF2A-knockout hippocampal neurons. (*A*) Schematic of the knockdown vector design (*Upper*) and its effects (*Lower*). GFP and microRNA (miR) cassette were expressed by the CMV promotor and polyA signal from Thymidine kinase (TK pA). Negative control (N.C.) and miRNA vectors were transfected, incubated for 3 d and analayzed by Western blot. Numbers under the Western blot data indicate the relative intensities of the Western blot experiment. (*B–D*) Inhibition of PIPKα or KIF2A resulted in elongated collateral branches in hippocampal neurons. Cells were transfected by the negative control vector or the miRNA vector (PIPKαKD) using electroporation when they were plated, cultured for 3 d, fixed, and observed by GFP signals. (*B*) Representative images of hippocampal neurons. (Scale bars, 100 μm.) (*C*) The number of collaterals longer than 50 μm was counted per 100 μm-long axons. Data are shown as mean ± SD; *P < 0.01, Student's t test; 30 neurons from three independent mice. (*D*) The total lengths of axons were calculated. Data are shown as mean ± SD; *P < 0.01, Student's t test; 30 neurons from three independent mice.
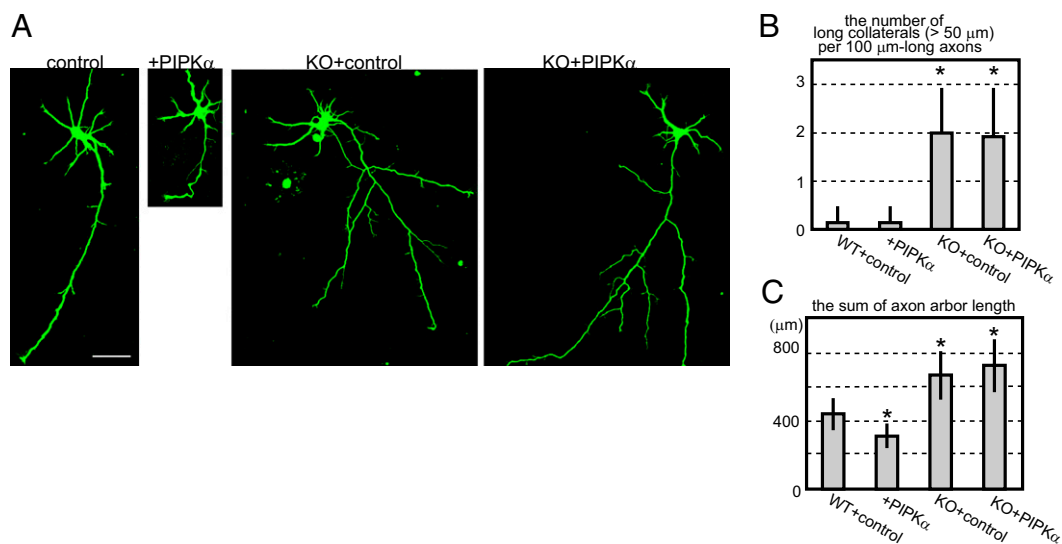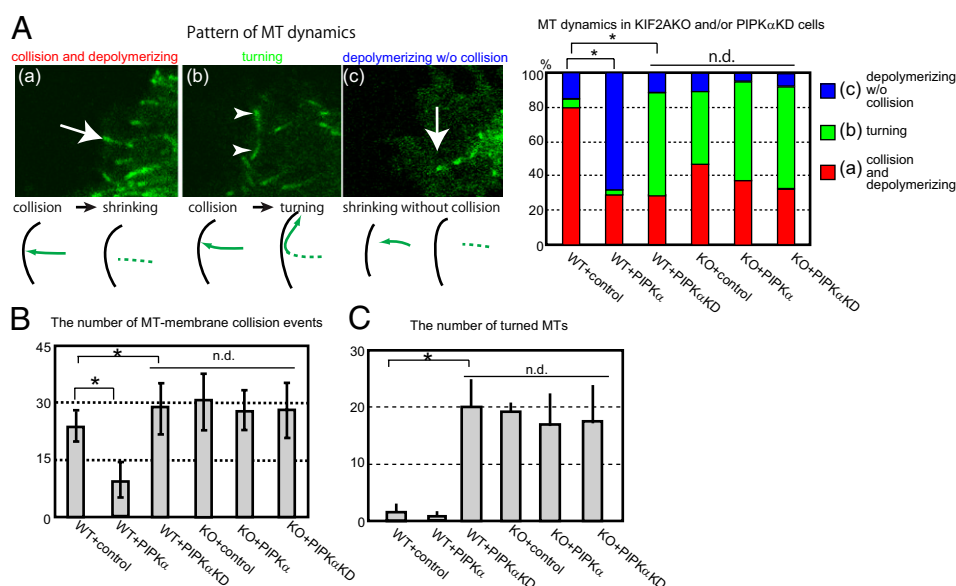
Noda et al.

Fig. 5. Overexpression of PIPKα in WT and *Kif2a⁻/⁻* neurons. WT or *Kif2a⁻/⁻* hippocampal neurons were transfected by GFP and either CFP (control) or CFP-PIPKα (+PIPKα) vectors at 2 d using a Ca^{2+}-phosphate method, cultured for 1 d, and observed by GFP signals. (*A*) Representative images of each cell. (Scale bar, 50 μm.) (*B*) The number of collaterals longer than 50 μm was counted per 100 μm-long axons. Data are shown as mean ± SD; *$P < 0.01$, Student's *t* test; 13 neurons from four independent mice. (*C*) Total lengths of axons were calculated. Data are shown as mean ± SD; *$P < 0.01$, Student's *t* test; 12 neurons from four independent mice.

cones by the superresolution microscopy that takes advantage of TIRF. In vitro assays showed that PIPKα could enhance the MT depolymerization induced by KIF2A (Fig. 3). As PIPs were not included in the in vitro assay, this result suggests that PIP_2 production is not required for KIF2A activation. This is clearly different from the PIPK-dependent regulation of actin filaments, in which PIP_2 production is a key step. Further studies including structural biology are needed to determine precisely how PIPKα activates KIF2A and whether PIP_2 is not totally required for the activation of KIF2A in cells. Knockdown experiments in hippocampal neurons showed that loss of function of either PIPKα or KIF2A caused the same morphological phenotype: abnormal elongation of axon collaterals (Fig. 4). As PIPKα knockdown did not further induce collateral elongation in *Kif2a⁻/⁻* background, it

is suggested that PIPKα and KIF2A work in the same pathway. Consistent with this, overexpression of PIPKα, inhibiting axon elongation in WT neurons, did not change neuronal morphology in *Kif2a⁻/⁻* neurons (Fig. 5). Coexpression of both KIF2A and PIPKα showed stronger effects than that caused by overexpression of PIPKα only (Fig. S3). Thus, KIF2A and PIPKα demonstrate functional synergy. Furthermore, because PIPKα overexpression did not affect neuronal morphology in *Kif2a⁻/⁻* background (Fig. 5), KIF2A is suggested to be a downstream target of PIPKα. This is consistent with our in vitro data showing that PIPKα enhanced KIF2A-dependent MT destabilization (Fig. 3). Interestingly, overexpression of KIF2A only did not significantly change neurite length in N1E-115 cells (Fig. S3). This is probably because KIF2A is not the only downstream target of PIPKα. It is thought that not

Fig. 6. The effect of PIPKα overexpression and PIPKα knockdown in *Kif2a⁺/⁺* or *Kif2a⁻/⁻* background. WT and *Kif2a⁻/⁻* neurons were transfected with EGFP-EB3 and either ECFP (control), ECFP-PIPKα (PIPKα), or a PIPKα-miRNA vector excluding the GFP cassette (PIPαKD) at 2 div by the Ca^{2+}-phosphate method. (*A*) (*Left*) Photographs and schema indicate three patterns of MT dynamics: (a) collision and depolymerization, (b) turning, and (c) depolymerization without collision. Arrows indicate MTs immediately before catastrophe. Arrowheads indicate turned MTs. (*Right*) MT dynamics in indicated neurons were counted. *$P < 0.01$, n.d. (no difference) $P > 0.01$, χ^2 test; more than 20 neurons from four independent mice were used. (*B*) Statistical analysis of the number of GFP-EB3 collisions with the plasma membrane in 10 min. Data are shown as mean ± SD; *$P < 0.01$, n.d. $P > 0.01$, Student's *t* test; 12 neurons from four independent mice were used in each sample. (*C*) The number of turned MTs was coun-ted. Data are shown as mean ± SD; *$P < 0.01$, n.d. $P > 0.01$, Student's *t* test; 12 neurons from four independent mice were used. In *B* and *C*, statistically no changes were observed between PIPKα-knockdown WT neurons, *Kif2a⁻/⁻* neurons, PIPKα-overexpressed *Kif2a⁻/⁻* neurons, and PIPKα-knockdown *Kif2a⁻/⁻* neurons.

only MTs but also actin filaments need to be controlled by PIPKα when the elongation of axon branches is inhibited. In fact, many actin-binding proteins are reported to be controlled by PIPK through PIP$_2$ production (16–20). Collectively, this study suggests that the activation of KIF2A is not sufficient but is essential for the function of PIPKα.

Materials and Methods

Material lists and detailed methods are presented in *SI Materials and Methods*.

Identification of KIF2A-Binding Proteins. Cerebellum derived from ICR strain mice at postnatal day 7 were used. The S2 fraction was purified as described (33) and immunoprecipitated using 30 μg of anti-KIF2A antibody and protein A-conjugated MACS beads (Miltenyi Biotec). The eluted fraction was separated by SDS/PAGE. Bands were eluted from the gel, trypsinized, and loaded on a 4700 proteomic TOF/TOF analyzer (Applied Biosystems). MS/MS spectra were analyzed with the MASCOT search database (http://www.matrixscience.com/cgi/search_form.pl?FORMVER=2&SEARCH=MIS).

MT-Depolymerizing Assays. Recombinant proteins were purified from *E. coli* using glutathione Sepharose (GE Healthcare Japan) and TALON beads (Takara Clontech). MT-depolymerizing assays were performed using a previously described method (7, 27). The amounts of PIPKα were estimated by quantification of the corresponding nondegraded bands because these fractions contained constant amounts of degraded bands of PIPKα. Depolymerization assays were performed using GMPCPP-stabilized MTs. To determine the EC$_{50}$, 0–1,000 nM GST-KIF2A was incubated with 1 μM MTs (equivalent to 0.1 mg/mL MTs) in the presence of BSA, PIPKα, or PIPKγ. The data were plotted and fit to the four-parameter logistic equation (Eq. **1**) and the EC$_{50}$ was calculated using KaleidaGraph 4.0 software (Synergy), where Response is the amount of tubulin in the supernatant fraction, R_{min} is the baseline, R_{max} is the maximal response, X is the enzyme concentration, and H is the Hill slope:

$$\text{Response} = R_{min} + (R_{max} - R_{min}) / \left[1 + 10^{H \cdot \log(EC50/X)} \right]. \qquad [1]$$

Immunofluorescent Microscopy and PALM. Microscopy was done as described (34, 35). In short, cells were fixed with 4% paraformaldehyde and permeabilized with 0.1% Triton X-100. For conventional observations, Alexa-conjugated secondary antibodies were used. We observed the neurons under an LSM 510 confocal microscope (Carl Zeiss). For PALM observation, anti-KIF2A antibody was directly labeled with ATTO488 (ATTO-TEC). PIPKα was visualized by using an Alexa 647-labeled anti-goat antibody. PALM observation was conducted using the ELYRA P.1 prototype system (Carl Zeiss).

Supporting Information Summary. Fig. S1 shows the specificity of the anti-PIPKα antibody. Fig. S2 shows the effect of PIPKα in N1E-115 cells. Fig. S3 shows cooperative activity of PIPKα and KIF2A. Movies S1, S2, S3, S4, S5, and S6 show the dynamics of the plus end of MTs in WT neurons, PIPKα-overexpressing neurons, PIPKα-knockdown neurons, *Kif2a*$^{-/-}$ neurons, PIKα-overexpressing *Kif2a*$^{-/-}$ neurons, and PIPKα-knockdown *Kif2a*$^{-/-}$ neurons, respectively.

1. Moore A, Wordeman L (2004) The mechanism, function and regulation of depolymerizing kinesins during mitosis. *Trends Cell Biol* 14:537–546.
2. Lawrence CJ, et al. (2004) A standardized kinesin nomenclature. *J Cell Biol* 167(1): 19–22.
3. Howard J, Hyman AA (2007) Microtubule polymerases and depolymerases. *Curr Opin Cell Biol* 19(1):31–35.
4. Hirokawa N, Noda Y (2008) Intracellular transport and kinesin superfamily proteins, KIFs: Structure, function, and dynamics. *Physiol Rev* 88:1089–1118.
5. Walczak CE, Mitchison TJ, Desai A (1996) XKCM1: A *Xenopus* kinesin-related protein that regulates microtubule dynamics during mitotic spindle assembly. *Cell* 84(1): 37–47.
6. Noda Y, Sato-Yoshitake R, Kondo S, Nangaku M, Hirokawa N (1995) KIF2 is a new microtubule-based anterograde motor that transports membranous organelles distinct from those carried by kinesin heavy chain or KIF3A/B. *J Cell Biol* 129(1):157–167.
7. Desai A, Verma S, Mitchison TJ, Walczak CE (1999) Kin I kinesins are microtubule-destabilizing enzymes. *Cell* 96(1):69–78.
8. Hunter AW, et al. (2003) The kinesin-related protein MCAK is a microtubule depolymerase that forms an ATP-hydrolyzing complex at microtubule ends. *Mol Cell* 11:445–457.
9. Homma N, et al. (2003) Kinesin superfamily protein 2A (KIF2A) functions in suppression of collateral branch extension. *Cell* 114:229–239.
10. Di Paolo G, De Camilli P (2006) Phosphoinositides in cell regulation and membrane dynamics. *Nature* 443:651–657.
11. Santarius M, Lee CH, Anderson RA (2006) Supervised membrane swimming: Small G-protein lifeguards regulate PIPK signalling and monitor intracellular PtdIns(4,5)P$_2$ pools. *Biochem J* 398(1):1–13.
12. van den Bout I, Divecha N (2009) PIP5K-driven PtdIns(4,5)P$_2$ synthesis: Regulation and cellular functions. *J Cell Sci* 122:3837–3850.
13. Ishihara H, et al. (1996) Cloning of cDNAs encoding two isoforms of 68-kDa type I phosphatidylinositol-4-phosphate 5-kinase. *J Biol Chem* 271:23611–23614.
14. Ishihara H, et al. (1998) Type I phosphatidylinositol-4-phosphate 5-kinases. Cloning of the third isoform and deletion/substitution analysis of members of this novel lipid kinase family. *J Biol Chem* 273:8741–8748.
15. Loijens JC, Anderson RA (1996) Type I phosphatidylinositol-4-phosphate 5-kinases are distinct members of this novel lipid kinase family. *J Biol Chem* 271:32937–32943.
16. Divecha N, et al. (2000) Interaction of the type Iα PIPkinase with phospholipase D: A role for the local generation of phosphatidylinositol 4,5-bisphosphate in the regulation of PLD2 activity. *EMBO J* 19:5440–5449.
17. Hernández-Deviez DJ, Roth MG, Casanova JE, Wilson JM (2004) ARNO and ARF6 regulate axonal elongation and branching through downstream activation of phosphatidylinositol 4-phosphate 5-kinase α. *Mol Biol Cell* 15(1):111–120.
18. Honda A, et al. (1999) Phosphatidylinositol 4-phosphate 5-kinase α is a downstream effector of the small G protein ARF6 in membrane ruffle formation. *Cell* 99:521–532.
19. van Horck FP, Lavazais E, Eickholt BJ, Moolenaar WH, Divecha N (2002) Essential role of type Iα phosphatidylinositol 4-phosphate 5-kinase in neurite remodeling. *Curr Biol* 12:241–245.
20. Yamazaki M, et al. (2002) Phosphatidylinositol 4-phosphate 5-kinase is essential for ROCK-mediated neurite remodeling. *J Biol Chem* 277:17226–17230.
21. Friedman DS, Vale RD (1999) Single-molecule analysis of kinesin motility reveals regulation by the cargo-binding tail domain. *Nat Cell Biol* 1:293–297.
22. Maney T, Wagenbach M, Wordeman L (2001) Molecular dissection of the microtubule depolymerizing activity of mitotic centromere-associated kinesin. *J Biol Chem* 276: 34753–34758.
23. Ovechkina Y, Wagenbach M, Wordeman L (2002) K-loop insertion restores microtubule depolymerizing activity of a "neckless" MCAK mutant. *J Cell Biol* 159:557–562.
24. Ogawa T, Nitta R, Okada Y, Hirokawa N (2004) A common mechanism for microtubule destabilizers—M type kinesins stabilize curling of the protofilament using the class-specific neck and loops. *Cell* 116:591–602.
25. Ems-McClung SC, Hertzer KM, Zhang X, Miller MW, Walczak CE (2007) The interplay of the N- and C-terminal domains of MCAK control microtubule depolymerization activity and spindle assembly. *Mol Biol Cell* 18:282–294.
26. Cooper JR, Wagenbach M, Asbury CL, Wordeman L (2010) Catalysis of the microtubule on-rate is the major parameter regulating the depolymerase activity of MCAK. *Nat Struct Mol Biol* 17(1):77–82.
27. Hertzer KM, et al. (2006) Full-length dimeric MCAK is a more efficient microtubule depolymerase than minimal domain monomeric MCAK. *Mol Biol Cell* 17:700–710.
28. Stepanova T, et al. (2003) Visualization of microtubule growth in cultured neurons via the use of EB3-GFP (end-binding protein 3-green fluorescent protein). *J Neurosci* 23: 2655–2664.
29. Hirokawa N, Niwa S, Tanaka Y (2010) Molecular motors in neurons: Transport mechanisms and roles in brain function, development, and disease. *Neuron* 68: 610–638.
30. Zhou R, Niwa S, Homma N, Takei Y, Hirokawa N (2009) KIF26A is an unconventional kinesin and regulates GDNF-Ret signaling in enteric neuronal development. *Cell* 139: 802–813.
31. Moore AT, et al. (2005) MCAK associates with the tips of polymerizing microtubules. *J Cell Biol* 169:391–397.
32. Doughman RL, Firestone AJ, Wojtasiak ML, Bunce MW, Anderson RA (2003) Membrane ruffling requires coordination between type Iα phosphatidylinositol phosphate kinase and Rac signaling. *J Biol Chem* 278:23036–23045.
33. Niwa S, Tanaka Y, Hirokawa N (2008) KIF1Bβ- and KIF1A-mediated axonal transport of presynaptic regulator Rab3 occurs in a GTP-dependent manner through DENN/MADD. *Nat Cell Biol* 10:1269–1279.
34. Nakata T, Niwa S, Okada Y, Perez F, Hirokawa N (2011) Preferential binding of a kinesin-1 motor to GTP-tubulin-rich microtubules underlies polarized vesicle transport. *J Cell Biol* 194:245–255.
35. van de Linde S, Sauer M, Heilemann M (2008) Subdiffraction-resolution fluorescence imaging of proteins in the mitochondrial inner membrane with photoswitchable fluorophores. *J Struct Biol* 164:250–254.

Noda et al.